Comparative Analysis of Simulation-Based Methods for Deriving the Phase- and Gain-Margins of Feedback Circuits With Op-Amps

Marius Neag, *Member, IEEE*, Raul Oneţ, István Kovács, and Paul Mărtari

***Abstract*—Ten methods for finding through simulations the small-signal phase and gain margins of feedback circuits based on op-amps are described and analyzed in this mostly tutorial paper. The testbenches employed by these methods are presented and the corresponding analytical expressions of the return ratio are derived and compared against their "ideal" counterpart, obtained with standard circuit analysis; the requirement that the return ratio should not depend on the point it was measured at is also verified. These analyses are performed on a fairly general case: a generic reciprocal two-port network that closes a feedback loop around an op-amp acting as the forward amplifier. The four main types of op-amps were considered. The limitations of some of the tested methods are then highlighted by simulations. Besides the detailed analysis of previously reported methods, the paper proposes a novel method for deriving the return ratio of feedback circuits, that employs only current stimuli; it is demonstrated analytically that this method can be used for bilateral circuits, not only for op-amp-based (unilateral) ones. Also, a recent method for deriving directly the phase margin of a circuit is extended to estimating the gain margin, too. Conclusions on the accuracy and suitability of the analyzed methods for practical circuit cases are drawn. These results are then extended to other circuit topologies.**

***Index Terms*—Phase and gain margins, return ratio, stability.**

I. Introduction

NEGATIVE feedback is a key concept in circuit design, widely used to obtain reliable transfer functions by minimizing the effects of parameter variations and external perturbations, to reduce nonlinearities and to improve the input/output impedances [1]–[4]. Feedback systems can be unstable, so ensuring their stability is a major design concern.

The Rosenstark theorem shows that the small-signal closed-loop gain of a feedback system depends on its return ratio [2]:

$$H_{CL} = H_\infty \cdot \frac{T}{1+T} + \frac{G_0}{1+T} \tag{1}$$

where T is the return ratio of the circuit, H_{CL} is the closed loop small-signal gain, G_0 is called the direct transmission term, $G_0 = H_{CL/T=0}$ and $H_\infty = H_{CL/T\to\infty}$ is the ideal closed-loop gain [3].

$T \to -1$ yields a mathematical singularity that indicates the instability of a physical circuit. As the return ratio T is a frequency-dependent function, two scalar conditions must be met simultaneously for this condition to occur:

$$T(f) = -1 \Rightarrow |T| = 1 \; and \; \varphi(T) = -180^\circ \tag{2}$$

Thus, the stability of a feedback circuit operating at a given DC operating point can be assessed by calculating its phase- and gain (module)-margins; these metrics indicate how close the circuit is from meeting the conditions above [3].

The classical feedback theory is based on two-port analysis of the forward amplifier—with the unilateral gain a—and its feedback network—with the unilateral reverse transmission factor f. The closed-loop gain of the circuit is given by:

$$H_{CL} = \frac{a}{1+a\cdot f} = \frac{1}{f}\cdot\frac{a\cdot f}{1+a\cdot f} \tag{3}$$

Thus, the critical condition for instability is $a \cdot f \to -1$, where the product of a and f is called the loop gain [3], [4]. This approach is relatively easy to follow in analytical analyses and provides the expressions of the input and output impedances. However, it does not cover all feedback topologies and can yield different loop gain values for a given circuit, when the type and location of signal sources applied to the circuit changes, even if the source-free circuit does not change [5]. Moreover, it is difficult to use for finding the loop gain through simulations performed on real-life circuits, which are usually far from the unilateral model described above [6].

The return ratio associated with a dependent source [1] and (1) are better suited for analyzing feedback circuits: they are independent on the feedback topology and do not depend on the type and location of the input sources. In fact, the forward amplifier does not need to be identified, and it is not assumed to be unilateral. Most importantly, the return ratio can be measured accurately experimentally and by simulations [7]–[9]. Difficulties can arise when this concept is employed for circuits comprising more than one controlled source [10] but this is not the case for the circuits discussed in this paper.

In general, the return-ratio differs from the loop gain [5] but both can be used to check the stability of feedback circuits based on the phase- and gain (module)-margins [1], [3]: it was demonstrated analytically that, although the return ratio and the loop gain of an op-amp-based circuit similar to the ones analyzed here have different expressions, they reach the value of -1, critical for stability, for exactly the same conditions [10].

This paper analyzes several methods for finding the return ratio, T, of feedback circuits based on voltage- and current-mode op-amps through the small signal SPICE-type simulations, AC, and S-parameter. The loop gain is no further discussed in this paper so there should be no confusion.

Manuscript received June 10, 2014; revised October 22, 2014; accepted October 24, 2014. Date of publication December 05, 2014; date of current version February 23, 2015. This paper was recommended by Associate Editor A. M. A. Ali.

The authors are with the Faculty of Electronics, Telecommunication and Information Technology, Basis of Electronics Department, Technical University of Cluj-Napoca, CJ RO-400027 Romania (e-mail: Marius.Neag@bel.utcluj.ro; Raul.Onet@bel.utcluj.ro; Istvan.Kovacs@bel.utcluj.ro; Paul.Martari@bel.utcluj.ro).

Digital Object Identifier 10.1109/TCSI.2014.2370151

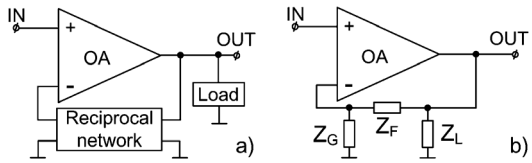

Fig. 1. (a) Circuit with a generic op-amp as the basic amplifier and a reciprocal network closing a classical series-shunt feedback loop; (b) the same circuit, with the feedback and load replaced by an equivalent Π network.

Section II describes the methodology used to analyze the methods considered here. It comprises the analysis of both the analytical expressions of T yielded by these methods and of simulations run on particular circuits. A fairly general case is considered: a generic reciprocal two-port network (a class which includes all passive networks) that closes a feedback loop around an op-amp, as shown on Fig. 1(a). Four main types of op-amps are considered for the forward amplifier: the traditional (V-V) op-amp, the current-feedback op-amp (CFBOA), the transconductance op-amp (OTA), and the current-current op-amp with asymmetric inputs, a particular case of which is the second-order current conveyor (CCII).

Sections III and IV present briefly the methods for finding T of unilateral, respectively bilateral, feedback circuits through measurements or simulations introduced by Middlebrook [7], [11], Rosenstark [8], Tian [12], and Ochoa [13], as well as a method based on the S-parameters analysis popular with RF designers. A novel method inspired by Ochoa's approach is also presented: it employs only current stimuli and its validity for bilateral feedback circuits was demonstrated analytically. A recently proposed method that yields directly the phase margin of a feedback circuit [14] is also described in Section IV, along with a proposed extension to gain-margin derivation. Section V presents two approximate methods for finding T popular within the industry due to their simplicity.

Section VI analyses comparatively the methods described before when applied to circuits derived from the general one shown in Fig. 1(a), considering each of the four op-amp types mentioned above as the basic amplifier. Employing these methods to the analysis of other circuit classes, which have multiple inputs and differential inputs and outputs, is discussed in Section VII. Section VIII summarizes the results and draws conclusions based on analytical analyses and simulations.

II. Methodology for Comparing the Methods for Finding the Small-Signal Return-Ratio of OA-Based Circuits Through AC Sims Analyzed Here

The methods for finding T discussed here are analyzed considering both the analytical analysis performed on a fairly general circuit and simulations run on a particular circuit. First, the analytical expressions of T yielded by these methods for the circuit shown in Fig. 1(b)—derived from the one shown in Fig. 1(a) by replacing the feedback network with its equivalent Π network and including the load into Z_L—are derived, considering the standard op-amp models presented in Fig. 2. These expressions are compared against the ideal ones yielded by the procedure introduced in [1], called hereafter T_{Bode}:

— One of the controlled sources (usually used to model active elements) is chosen; its output is disconnected from the circuit and an independent test source of the same type and sign is used to drive that circuit node or loop instead. The controlled source maintains its coupling to the controlling element.

— T results as the ratio between the signal that appears at the output of the controlled source and the test signal, generated by the independent source that replaced it in the circuit [3].

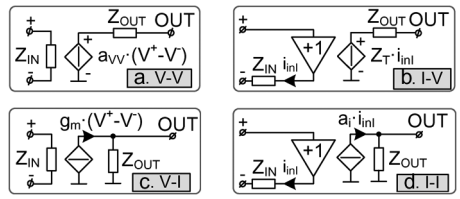

Fig. 2. Simple models of the four types of op-amps, used to derive the return ratio expressions analytically: (a) V-V op-amp; (b) CFB-OA; (c) OTA (transconductance OA); (d) current-current op-amp with asymmetric inputs.

The compliance with the requirement that T should not depend on the point it was measured at is also verified: each method for deriving T is applied twice, once at the input and once at the output of the op-amp. Another general requirement is that the DC operating point (OP) of the circuit is preserved during all the tests/simulations required. The limitations and shortcomings of some of the methods compared here are demonstrated through simulations for a show-case circuit.

III. General Methods for Finding the Return Ratio of Unilateral Feedback Circuits Through Simulations

This section presents briefly three general methods for finding the return ratio of feedback circuits through measurements or simulations, introduced in [7] and [8]. They share two key features: i) they are independent of the test point and ii) if used to derive the analytical expression of the return ratio they yield the accurate expression, T_{Bode}.

A. Middlebrook's Method for Finding the Return Ratio

Of the four methods for measuring the return ratio of feedback circuits through measurements proposed in [7] the third has been used the most for finding T through small-signal simulations. It consists of successively injecting voltage and current test signals into an arbitrary-chosen point of the loop.

Fig. 3 illustrates this method: the Norton model shown within the dotted-line rectangle represents, without loss of generality, any circuit with unilateral feedback [7], [12]; the voltage injection shown in Fig. 3(a) is used to compute the voltage return ratio, T_V, while Fig. 3(b) presents the current injection which yields the current return ratio, T_I. The two return ratios are derived by using the following formulae:

$$T_V = -\frac{v_Y}{v_X}; T_I = -\frac{i_Y}{i_X}. \tag{4}$$

The return ratio of the circuit results by combining T_V and T_I:

$$\frac{1}{1+T} = \frac{1}{1+T_V} + \frac{1}{1+T_I}; T = \frac{T_V \cdot T_I - 1}{T_V + T_I + 2}. \tag{5}$$

Fig. 4 presents the test configurations for finding the return ratio of the circuit in Fig. 1(b) through AC simulations [7].

Using the model shown in Fig. 3, in [7] it was demonstrated that this method—called here the Middlebrook's method—is valid for circuits with unilateral feedback networks and that it is not dependent on the chosen test point (for example, it yields exactly the same result if the loop is broken between points marked

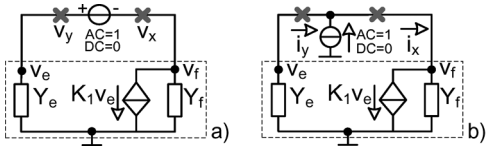

Fig. 3. Test configurations for Middlebrook's method applied to a general model of circuits with unilateral feedback: (a) voltage injection and (b) current injection—for deriving the voltage and current return ratios defined by equation (4).

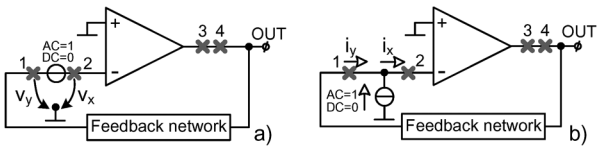

Fig. 4. Test configurations for applying Middlebrook's method to the circuit shown in Fig. 1: (a) circuit for deriving T_V and (b) circuit for deriving T_I.

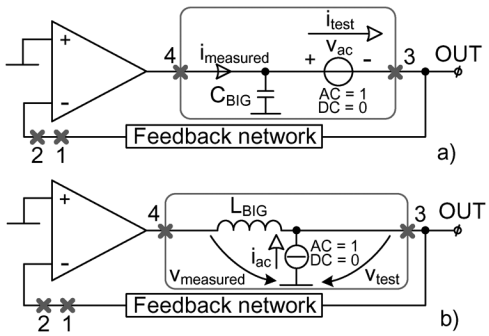

Fig. 5. Test configurations required by Rosenstark's method [15], [16]: (a) Circuit for deriving T_I^*; (b) Circuit for deriving T_V^*. Breaking the loop at other points, e.g., 1–2, will yield—after applying Equation (7)—exactly the same T.

1–2 or the points marked 3–4). The injection of test signals does not change the node impedances of the circuit but the post-processing required to derive T from the return ratios obtained through simulations or measurements (T_V and T_I) demands the addition/subtraction of units, making this method susceptible to numerical inaccuracies [7], [8].

B. Rosenstark's Method for Finding the Return Ratio

This problem is avoided by the method for measuring the return ratio introduced in [8], called here the Rosenstark's method. It can be easily adapted to the task of finding T of the Fig. 1(b) circuit through AC simulations [15], [16]: the current- and voltage-ratios defined in [8] are determined by using the configurations shown in Fig. 5(a) and Fig. 5(b)., respectively:

$$T_I^* = -\frac{i_{measured}}{i_{test}},\ T_V^* = -\frac{v_{measured}}{v_{test}} \tag{6}$$

These transfer ratios are different from the ones defined by the Middlebrook's method; consequently, the return ratio of the circuit results from an expression different from (5):

$$\frac{1}{T} = \frac{1}{T_V^*} + \frac{1}{T_I^*};\ T = \frac{T_V^* \cdot T_I^*}{T_V^* + T_I^*}. \tag{7}$$

The inductor $\mathrm{L_{BIG}}$ and the capacitor $\mathrm{C_{BIG}}$ have values large enough to act as open-circuit, respectively short-circuit in small-signal simulations, over the entire frequency range of interest; thus the loop is broken in AC. In DC they operate as short- respectively open-circuits so the OP of the circuit is preserved. It was demonstrated in [8] that this method yields theoretically accurate results for circuits with unilateral feedback networks, irrespective of the chosen test point.

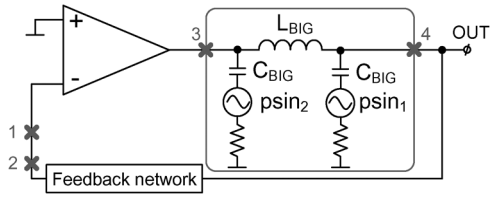

Fig. 6. Test configuration for finding T by using the S-parameters method.

C. Finding T by Using S-Parameters Simulations

A method for finding T that circulates within the community of RF designers is presented in Fig. 6. The loop is broken by inserting an inductor with very large value, $\mathrm{L_{BIG}}$; the stimulus is provided by a port and another port is used to measure the resulting signal—ports $\mathbf{psin_1}$ and $\mathbf{psin_2}$ in Fig. 6, respectively. These ports are connected to the $\mathrm{L_{BIG}}$ terminals through very large capacitors, $\mathrm{C_{BIG}}$. T is then derived by combining the Y parameters provided by an S-parameter simulation, as follows:

$$T_{SParam} = -Y_{21}/\left(\frac{Y_{22}+Y_{11}}{1+Y_{12}/Y_{11}} - \frac{Y_{12}\cdot Y_{21}}{Y_{11}+Y_{12}} + \frac{Y_{12}\cdot Y_{11}}{Y_{11}+Y_{22}}\right) \tag{8}$$

The usual S- to Y-parameters relationships are to be used:

$$\begin{aligned} &Y_{11} = ((1+S_{22})\cdot(1-S_{11}) + S_{12}\cdot S_{21}))\,/Denom_S;\\ &Y_{12} = -2\cdot S_{12}/Denom_S; Y_{21} = -2\cdot S_{21}/Denom_S;\\ &Y_{22} = ((1+S_{11})\cdot(1-S_{22}) + S_{12}\cdot S_{21})/Denom_S;\\ &Denom_S = (1+S_{11})\cdot(1+S_{22}) - S_{12}\cdot S_{21}. \end{aligned} \tag{9}$$

The main advantage of this method—called hereafter the "S-params" method—is that the impedances of the two ports can be set by the user as to best fit the circuit. This way, one can accommodate amplifiers designed to operate with well defined loads, as it is often the case in RF systems. Also, only one simulation is needed for deriving the return ratio of the circuit.

One can prove analytically that this method is independent on the point the feedback loop is broken and that it is accurate for circuits with unilateral feedback networks, represented by the unilateral model shown in Fig. 3, irrespective of the impedance set by the user for the ports $\mathbf{psin_1}$ and $\mathbf{psin_2}$.

IV. General Methods for Finding the Return Ratio of Bilateral Feedback Circuits Through Simulations

A. Tian's Method for Finding the Return Ratio of Bilateral Feedback Circuits—The Basis of Cadence's STB Analysis

Cadence's Virtuoso Analog Design Environment comprises a dedicated tool for finding the return ratio of single-loop feedback circuits, called the Stability Analysis (STB) [17]. The user is only asked to break the feedback loop by inserting an independent voltage source with $\mathrm{V_{DC}} = 0$ and $\mathrm{V_{AC}} = 0$.

The STB analysis is independent on the point within the loop the voltage source is inserted. It provides the return ratio magnitude and phase characteristics without any (visible to user) post-processing. It can be applied to fully differential circuits as well; in that case the differential feedback loops are broken by using a dedicated cell, called diffstbprobe.

Reference [17] gives no theoretical background for the STB analysis but it very likely employs the loop-based two-port and the device-based gain-nulling algorithms presented in [12]. The later deals with a case not discussed here: local feedback loops not directly accessible to the designer, such as those formed around a MOS transistor by its own parasitic elements.

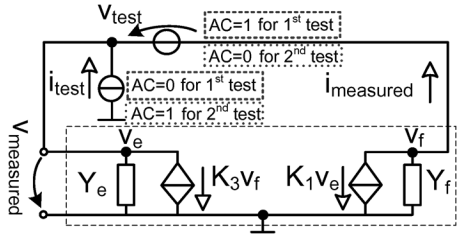

Fig. 7. The general bilateral model of a feedback circuit is shown within the dotted-line rectangle; the sources $\mathbf{v_{test}}$ and $\mathbf{i_{test}}$ are activated successively to derive the terms employed in Equation (10) to obtain the return ratio of the circuit.

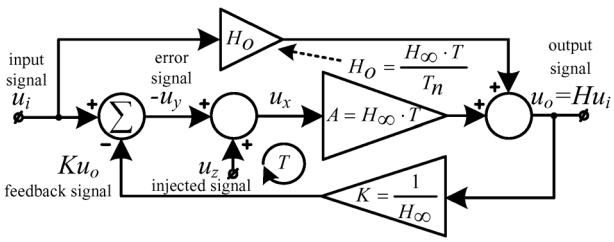

Fig. 8. The equivalent block diagram of a bilateral circuit used by the GFT.

The loop-based two-port algorithm deals with single-loop feedback circuits as those analyzed here. It is similar with the Middlebrook's method presented in Section III-A as it, too, requires that a voltage and a current test signals are injected successively at arbitrary chosen points of the loop. However, it does not rely on voltage- and current- return ratios but makes use of both the voltages and currents yielded by each test.

This method is accurate for general feedback circuit, with bilateral transmissions, that can be modeled as shown in Fig. 7, within the dotted-line rectangle. Two AC simulations are run, each with only one of the small-signal $\boldsymbol{v_{test}}$ and $\boldsymbol{i_{test}}$ test sources active. The current and voltage resulting from each simulation, denoted $\mathbf{i_{measured}}$ and $\mathbf{v_{measured}}$ in Fig. 7, are used to obtain T:

$$\begin{aligned} A &= i_{measured}|_{i_{test}=1}^{v_{test}=0};\ C = v_{measured}|_{i_{test}=1}^{v_{test}=0};\\ B &= i_{measured}|_{i_{test}=0}^{v_{test}=1};\ D = v_{measured}|_{i_{test}=0}^{v_{test}=1};\\ T &= \frac{AD-BC-A}{2(BC-AD)+A-D+1} = \frac{k_1+k_3}{Y_e+Y_f}. \end{aligned} \tag{10}$$

B. Middlebrook's General Feedback Theorem

The General Feedback Theorem (GFT) introduced in [11] is based on the dissection theorem, that allows it to model a bilateral feedback circuit as shown in Fig. 8. The closed-loop gain of the circuit results by combining "second-level" transfer functions obtained by injecting test signals in such a way that particular signals within the circuit are nulled:

$$\begin{aligned} H_{CL} &= H_\infty \cdot \frac{1+1/T_n}{1+1/T_{GFT}}\\ &= H_\infty \cdot \frac{T_{GFT}}{1+T_{GFT}} + H_0 \cdot \frac{1}{1+T_{GFT}};\\ H_\infty &= u_O/u_I|_{u_Y=0};\\ T_{GFT} &= u_Y/u_X|_{u_I=0}; T_n = u_Y/u_X|_{u_O=0}. \end{aligned} \tag{11}$$

If the test signal is applied at the error summing point of the feedback topology—denoted Σ in Fig. 8—the "second-level" transfer functions have useful physical meaning: e.g., H_∞ is the ideal closed-loop gain, which results when the error signal is nulled (equivalent to the loop having infinite gain). The critical condition for instability is $T_{GFT} = -1$, and the usual phase- and gain-margin stability metrics can be employed in respect to it.

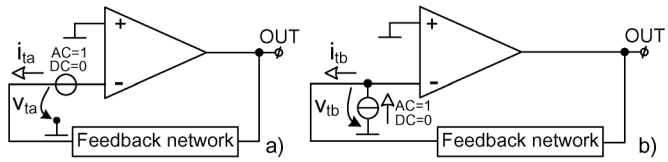

Fig. 9. Test configurations for finding T_{GFT}, associated with the GFT concept.

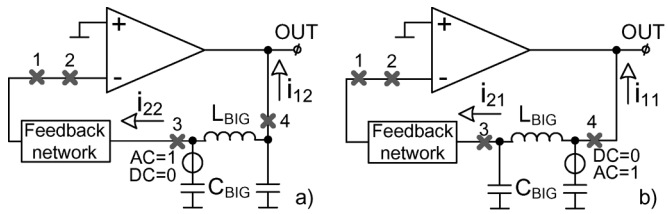

Fig. 10. Test configurations for Ochoa's method, that yield the terms used by Equation (13): (a) circuit for deriving currents i_{22} and i_{12} and (b) circuit for i_{11} and i_{21}.

Despite the obvious similarity between (1) and (11) the T_{GFT} in (11) is not necessarily equal to the return ratio of the circuit; in fact, its expression depends on the injection point of the test signal. However, the conditions for which $T_{GFT} = -1$ are precisely the ones for which $T = -1$; thus one obtains the same phase- and gain-margin values when using T_{GFT} as if using T.

The GFT concept was further developed in [11] by using a voltage and a current source to inject simultaneously two test signals in the circuit in such a way that pairs of resulting signals are nulled. This complicates the procedure but provides in-depth analysis of the closed-loop gain of the circuit, highlighting the factors that degrade its ideal form, H_∞. A user-friendly implementation was integrated into Intusoft's ICAP/4.

Simpler analysis methods based on the GFT approach were developed for various SPICE-compatible simulators [18]. For example, one can use the same test configuration as for the Middlebrook's method presented in Fig. 4 but monitor (then use to derive T_{GFT}) more of the resulting currents and voltages. This method is defined by Fig. 9 and (12).

$$T_{GFT} = \frac{v_{ta}\cdot i_{tb} - v_{tb}\cdot i_{ta}}{v_{tb}\cdot i_{ta} - v_{ta}\cdot i_{tb} - 1} \tag{12}$$

C. Ochoa's Method for Finding the Return Ratio

Recently, another accurate method for finding T was developed by using the Driving Point approach [13]. Fig. 10 presents a version of the test configurations required by this method when applied to the circuit shown in Fig. 1; each one yields a pair of currents, which are then combined to obtain T:

$$T = -\frac{i_{12}+i_{21}}{i_{11}+i_{22}} \tag{13}$$

Note that the op-amp output is effectively shorted to ground for the test shown in Fig. 10(a), while for the test shown in Fig. 10(b) it is driven directly by the test source. If this is not convenient one can break the loop in another place, such as at points 1–2. However, in this case the inverting input of the op-amp will be shorted to ground or driven by the test source.

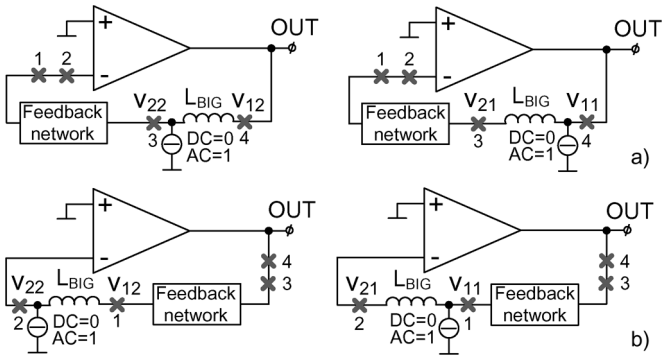

Fig. 11. Test configurations for deriving the terms used by Equation (14) to obtain T: The current-only stimuli can be applied at the op-amp output (a) or input (b).

D. Finding the Return Ratio by Using Only Current Stimuli

Fig. 11 shows the testbenches required by a novel method for deriving the return ratio of the circuit shown in Fig. 1, inspired by Ochoa's approach [13] discussed in Section IV-C. Similar to Ochoa's method, the feedback loop is broken by inserting a large inductor, $\mathrm{L_{BIG}}$, and T results by combining signals obtained by applying test sources successively to each terminal of $\mathrm{L_{BIG}}$. The main difference is that the proposed method employs only current stimuli—the current sources with $\mathrm{DC} = 0$, $\mathrm{AC} = 1$ shown in Fig. 11—and measures the resulting voltages at the $\mathrm{L_{BIG}}$ terminals. The T expression, independent on the point the feedback loop is broken at, is given by:

$$T = -\frac{v_{12} + v_{21}}{v_{11} + v_{22}} \tag{14}$$

By comparing Figs. 10 and 11 one notices that the proposed method employs simpler testbenches than Ochoa and does not require the op-amp output or inverting input to be grounded.

Let us demonstrate analytically that this method yields the correct expression for the return ratio of a general feedback circuit—that is, without the restriction of having an unilateral feedback network that limits Middlebrooks's and Rosenstark's methods—irrespective of the chosen test point. The general circuit can be represented by the bilateral model shown in Fig. 12 within the dotted-line rectangle [12]. First, the AC current source $\mathbf{i_{test}}$ is applied to node 3, as shown in Fig. 12(a), and the resulting voltages $\mathbf{v_{12}}$ and $\mathbf{v_{22}}$ are recorded. Next, the AC current source $\mathbf{i_{test}}$ is applied to node 4, as shown in Fig. 12(b), and the resulting currents $\mathbf{v_{21}}$ and $\mathbf{v_{11}}$ are recorded. The inductors $\mathrm{L_{BIG}}$ have values large enough to act as effective open-circuits in small-circuit analysis. Thus, the expressions of the currents mentioned above can be written as follows:

$$\begin{aligned}
\lim_{L_{BIG}\to\infty} v_{11} &= -\frac{Y_e}{k_1 k_3 - Y_e Y_f};\\
\lim_{L_{BIG}\to\infty} v_{12} &= \frac{k_1}{k_1 k_3 - Y_e Y_f};\\
\lim_{L_{BIG}\to\infty} v_{21} &= \frac{k_3}{k_1 k_3 - Y_e Y_f};\\
\lim_{L_{BIG}\to\infty} v_{22} &= -\frac{Y_f}{k_1 k_3 - Y_e Y_f}.
\end{aligned} \tag{15}$$

The T expression is obtained by applying (14):

$$T = -\frac{v_{12} + v_{21}}{v_{11} + v_{22}} = \frac{k_1 + k_3}{Y_e + Y_f} \tag{16}$$

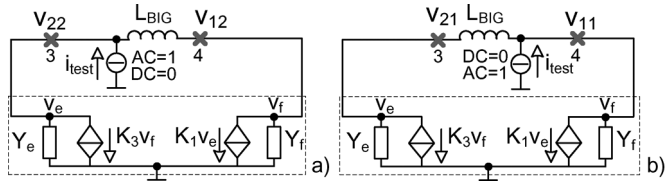

Fig. 12. Applying the proposed method for finding T to a general feedback circuit represented by the bilateral model shown within the dotted rectangles.

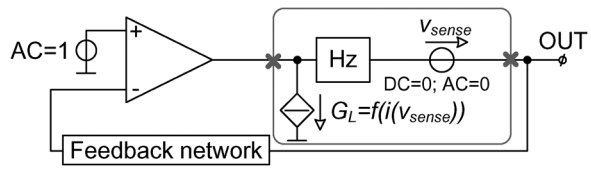

Fig. 13. Test configuration for von Wangenheim's method. The block $\mathbf{H_z}$ introduces an additional phase shift in the loop, with the value set by the user. The controlled current source $\mathrm{G_L}$ restores the loading of the op-amp output.

As this is exactly the "ideal" T expression obtained by direct circuit analysis, the demonstration is complete.

By using this approach one can demonstrate that Ochoa's method yields the correct expression for the return ratio of any feedback circuit that can be modeled as shown in Fig. 7.

E. Von Wangenheim's Method for Determining the Phase Margin Without Breaking the Feedback Loop

Reference [14] proposes a novel method for finding the phase margin of a feedback amplifier, without determining the return ratio of the feedback loop. It is based on the fact that the closed-loop phase-frequency characteristic exhibits a phase step of 180° if the phase margin drops below zero.

The phase margin of the system is forced to cross the zero point by injecting additional phase shifts into the feedback loop. This is achieved by inserting an analog behavioral block, $\mathrm{H_z}$, with the transfer function $H_Z(s) = e^{-j\varphi_Z}$. The output impedance of the block $\mathrm{H_z}$ is nil. In order to maintain the current loading at the op-amp output, the test configuration shown in Fig. 13 also comprises the current source $\mathrm{G_L}$; this replicates the output current of $\mathrm{H_z}$ (sensed through the voltage source $\mathrm{V_{sense}}$) but with the phase shift introduced by $\mathrm{H_z}$ reverted: $G_L(s) = i(v_{sense})e^{+j\varphi_Z}$. This way, although the insertion of the block $\mathrm{H_z}$ breaks the feedback loop, the controlled source $\mathrm{G_L}$ restores the loadings at the op-amp output not only in DC, but over the entire frequency range.

First, the designer needs to estimate (through experience, or hand calculations, etc.) the range of the phase margin and find two values for the phase shift to be introduced by $\mathrm{H_Z}$—called here $\varphi_{Z,1}$ and $\varphi_{Z,2}$—that will result in a positive and a negative value for the phase margin, both close to zero. AC simulations are run for these phase shifts and the resulting phase characteristics of the closed-loop response are monitored. In both cases, the slope of each phase characteristic will assume extreme values in the vicinity of the loop-gain cross-over frequency. The resulting peak values of the group delay, called hereafter $\tau_{GR1,peak}$ and $\tau_{GR2,peak}$, have opposite signs and are reliable measures of the "distance" between the respective injected phase shifts, $\varphi_{Z,1}$ and $\varphi_{Z,2}$, and the critical angle (equal to the phase margin) that defines the stability limit. The phase margin (PM) is obtained through interpolation, as follows:

$$PM = \frac{|\tau_{GR1,peak}| \cdot |\varphi_{Z,1}| + |\tau_{GR2,peak}| \cdot |\varphi_{Z,2}|}{|\tau_{GR1,peak}| + |\tau_{GR2,peak}|} \tag{17}$$

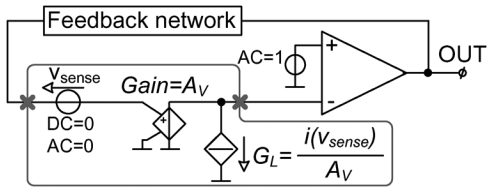

Fig. 14. Test configuration for the method for calculating the module margin derived from von Wangenheim's method. The VCVS allows the user to change the loop gain by A_V; $\mathrm{G_L}$ restores the loading of the feedback network.

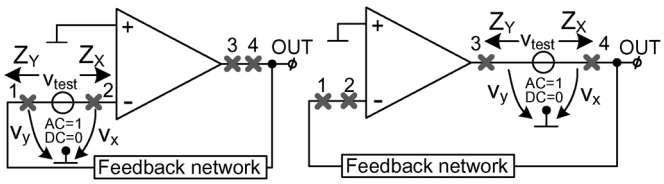

Fig. 15. Test configurations for the $\mathrm{V_{AC}}$ method: the loop is broken by inserting an independent voltage source, $\mathbf{v_{test}}$, with DC $= 0$, AC $= 1$, either at the input (points 1–2) or at the output (points 3–4) of the op-amp. $T = -v_y/v_x$.

The usefulness of this method is limited, as it provides no information on the gain margin. This can be overcome by using the following procedure: first, the block $\mathrm{H_z}$ is replaced by an ideal voltage-to-voltage amplifier with the programmable gain A_V and the current $\mathrm{G_L}$ is set to $i(v_{sense})/A_V$.

Next, the designer chooses two values for the gain, called here A_{V1} and A_{V2}, for which the circuit goes from a positive to a negative gain margin. AC simulations are run for these gains and the resulting peak values of the group delay, called here $\tau_{GR1,peak}$ and $\tau_{GR2,peak}$, are recorded. They indicate how close the gain of the loop gets to the critical value (i.e., the inverse of the gain margin [3]) that defines the stability limit. The gain margin results from an interpolation similar to (17), but the errors can be significant if the gains A_{V1} and A_{V2} are far apart.

Both the method for calculating the phase margin ((17)) and its extension for deriving the gain margin can be applied by inserting the block $\mathrm{H_z}$, respectively the voltage-voltage amplifier, at the input of the op-amp, as shown in Fig. 14.

The precision of this method for calculating the phase and the gain margin depends on the designer choosing properly the values for the phase shifts $\varphi_{Z,1}$ and $\varphi_{Z,2}$, respectively for the voltage gains A_{V1} and A_{V2}. In general, the chosen values should be as close to each other as possible, while forcing the corresponding phase/module margin to jump between a positive and a negative value. If the test values are far apart, the errors increase significantly, especially if the gain/phase margin goes negative while forcing a phase/module shift.

In practice, one has to run sets of AC simulations, iteratively reducing the width of the search range while adjusting its center value based on the phase and gain margin values obtained in the previous run. This method is not based on particular assumptions regarding the topology of the analyzed circuit, therefore it can be applied to any feedback circuit.

V. Approximate Methods Used in Industry for Finding the Return Ratio of Op-Amp-Based Feedback Circuits

A. The V_{AC} Simplified Method For finding T Through AC Sims

The first two methods for measuring the return ratio proposed in [7] show that, in certain conditions, each of the two return ratios defined by (4) can provide on its own an approximation of the overall T. The most popular version is illustrated in Fig. 15, and will be called here the $\mathrm{V_{AC}}$ method.

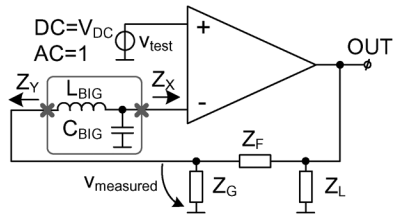

Fig. 16. Test configuration for the $\mathrm{L_{BIG}} - \mathrm{C_{BIG}}$ method: the loop is broken at the inverting input of the op-amp by inserting a large inductor, $\mathrm{L_{BIG}}$, then that input is shorted to ground by $\mathrm{C_{BIG}}$. T results as the ratio $\mathrm{v_{measured}}/\mathrm{v_{test}}$.

The feedback loop is broken by inserting an independent voltage source, $\mathbf{v_{test}}$, with DC $= 0$ and AC $= 1$, and T is derived as the ratio between the voltages developed at the terminals of this source. In order to increase the accuracy of this approximate method the loop has to be broken at such a point that the impedance seen at the $\mathbf{v_{test}}$ terminal looking forward around the loop is much greater than the impedance seen from the other $\mathbf{v_{test}}$ terminal looking backwards to the loop [7]:

$$T_{AC} = -\frac{v_y}{v_x} \cong T \text{ if } Z_X \gg Z_y \tag{18}$$

Depending on the op-amp type, the loop can be broken at the op-amp input or output, as indicated in Fig. 15 by points 1–2 and 3–4, respectively. The DC operating point of the circuit is not modified by the insertion of the independent voltage source, as in DC this source is equivalent to a short-circuit.

B. The $L_{Big} - C_{Big}$ Method for Finding T Through AC Simulations

Fig. 16 presents the test configuration of another simple, but approximate, method for finding T that requires only one AC simulation. The feedback is broken without impacting the DC operating point by simply inserting an inductor with a very large inductance, $\mathrm{L_{BIG}}$, in series with the inverting input of the op-amp. That input is then shorted to ground (for small-signal simulations) by a large capacitor, $\mathrm{C_{BIG}}$, placed there. Finally, an independent voltage source, $\mathbf{v_{test}}$, with AC $= 1$ and the appropriate DC level, $\mathrm{V_{DC}}$—the same DC level as the test signal source—is used to drive the noninverting input of the op-amp, disconnected from ground for this purpose. T is then simply read as the voltage that appears at the $\mathrm{L_{BIG}}$ terminal not connected to the op-amp—denoted $\mathbf{v_{measured}}$ in Fig. 16:

$$T = \frac{v_{measured}}{v_{test}} = v_{measured} \text{ if } v_{test} = 1 \tag{19}$$

An important shortcoming of the $\mathrm{L_{BIG}} - \mathrm{C_{BIG}}$ method is that the common-mode inverting input impedance of the op-amp, between its inverting input and ground, is short-circuited in AC sims by $\mathrm{C_{BIG}}$, therefore its influence on T will be ignored. Also, it cannot be applied to fully-differential circuits with topologies derived from the op-amp-based inverting amplifier.

VI. Comparing the Methods for Finding T Presented Here Through Analytical Analysis and Simulations

Let us start with the derivation of the accurate expression of the return ratio, T_{Bode}, by applying the standard procedure described in Section II to the circuit presented in Fig. 1(b), with the generic op-amp there replaced by the four models shown in

Fig. 2. The resulting expressions of the return ratios for the four op-amp types, respectively T_{Bode}^{v-v}, T_{Bode}^{i-v}, T_{Bode}^{v-i}, T_{Bode}^{i-i}, are:

$$T_{Bode}^{v-v}=\frac{a_{vv}Z_{IN}Z_LZ_G}{denom_T^{Bode}};\ T_{Bode}^{i-i}=\frac{a_iZ_LZ_GZ_{OUT}}{denom_T^{Bode}}$$
$$T_{Bode}^{i-v}=\frac{Z_TZ_LZ_G}{denom_T^{Bode}};\ T_{Bode}^{v-i}=\frac{g_mZ_{IN}Z_LZ_GZ_{OUT}}{denom_T^{Bode}} \quad (20)$$
$$\begin{aligned}denom_T^{Bode}=&Z_{IN}Z_LZ_F+Z_{IN}Z_LZ_G+Z_{IN}Z_LZ_{OUT}\\&+Z_{IN}Z_FZ_{OUT}+Z_{IN}Z_GZ_{OUT}\\&+Z_FZ_GZ_{OUT}+Z_LZ_FZ_G+Z_LZ_GZ_{OUT}\end{aligned}$$

Details on the derivation of these expressions and their expanded form can be found in a previous work of ours, [19].

Direct circuit analysis of the test configurations employed by the three methods described in Section III, shown in Figs. 4–6, yields precisely the return ratio expressions given by (20). Moreover, the same result is obtained whether the loop is broken at the input or output of the op-amp—between points 1–2 or 3–4 in Figs. 4–6, respectively. This is due to the fact that the circuits analyzed here are unilateral; in fact, this is the case for most practical cases of op-amp-based feedback circuits, where the large forward gain of the op-amp diminishes the effects other transmission factors may have.

The same results were obtained for the first four methods presented in Section IV, which can deal with bilateral feedback circuits, as well. The gain- and phase-margin values obtained by applying these methods to various feedback circuits were always matched (within the interpolation error) by those obtained by using von Wangenheim's method and its extension described in Section IV-E. Therefore, all methods presented in Sections III and IV will be called "accurate."

Direct circuit analysis performed on the test circuits required by the V_{AC} shown in Fig. 15 yield T expressions quite different from the accurate ones given by (20). Also, this method yields different expressions for the return ratio if the loop is broken at the op-amp input or output. However, the T expressions yielded by the V_{AC} method converge towards the accurate ones if the impedances Z_X and Z_Y shown in Fig. 15 meet the condition $Z_X \gg Z_Y$, as required by (18).

If the V_{AC} method is applied at the op-amp input (points 1–2 in Fig. 15) the expressions of impedances Z_X and Z_Y are:

$$Z_{X(1-2)}=Z_{IN};\ Z_{Y(1-2)}=Z_G\|[Z_F+Z_L\|Z_{OUT}] \quad (21)$$

If V_{AC} method is applied at the op-amp output one obtains:

$$Z_{X(3-4)}=Z_L\|[Z_F+Z_G\|Z_{IN}];\ Z_{Y(3-4)}=Z_{OUT} \quad (22)$$

The situation for the $L_{BIG}-C_{BIG}$ is very similar: the return ratio expressions obtained for the test circuit shown in Fig. 16 are generally different from the accurate ones given by (20). It can be demonstrated analytically that they converge towards the same expressions as T_{Bode} if the circuit meets a condition similar to the V_{AC} method case: $Z_X \gg Z_Y$, where impedances Z_X and Z_Y are defined as shown in Fig. 16. The similarity with the V_{AC} method applied at the op-amp input results in Z_X and Z_Y having the same expressions as in that case, i.e., (21).

Thus, one can decide if one of these "approximate" methods is suited to analyze a given circuit by simply assessing the degree the condition $Z_X \gg Z_Y$ is met by that circuit. This inequality must be maintained at least up to the highest of the frequency at which the module of T equals 1 ($F_{0\,dB}$) and the frequency at which the phase of T equals -180° (F_{-180°).

In general, the return ratio characteristics provided by these "approximate" methods are reasonably close to the accurate ones if the feedback network is purely resistive and the input impedance of the op-amp is very large (for the $L_{BIG}-C_{BIG}$ and the V_{AC} method applied at the op-amp input) or very small (for the V_{AC} method applied at the op-amp output). However, the differences can become dramatic if the feedback network includes frequency-dependent impedances, as is the case for most real-life circuits: for certain cases these methods can predict instability for circuits proven stable by the accurate methods while for other cases things go the other way around.

In the following section the limitations of the V_{AC} and $L_{BIG}-C_{BIG}$ methods are demonstrated through simulations run on a show-case circuit based on the V-V op-amp.

A. Feedback Circuits Based on Voltage-Voltage Op-Amps

1) Analytical Analysis: The return ratio expression obtained for the test circuit required by the $L_{BIG}-C_{BIG}$ method shown in Fig. 16 considering the V-V op-amp model from Fig. 2(a), is different from T_{Bode}^{v-v}:

$$\begin{aligned}T_{L_\infty C_\infty}^{v-v}&=\frac{a_{VV}Z_LZ_G}{Z_LZ_F+Z_LZ_G+Z_LZ_{OUT}+Z_FZ_{OUT}+Z_GZ_{OUT}}\\&=\frac{a_{VV}Z_LZ_G}{denom_{Z_Y}}\end{aligned} \quad (23)$$

They converge to the same expressions if the impedances Z_X and Z_Y shown in Fig. 16 meet the condition $Z_X \gg Z_Y$:

$$T_{Bode}^{v-v}=\frac{a_{VV}Z_LZ_G}{denom_{Z_Y}\cdot(1+Z_Y/Z_X)}\xrightarrow{Z_X\gg Z_Y}T_{L_\infty C_\infty}^{v-v} \quad (24)$$

Equations (21) and (24) suggest that the $L_{BIG}-C_{BIG}$ method can provide acceptable results only if the input impedance of the V-V OA is large enough over the required frequency range.

The analytical analysis of the test circuits required by the V_{AC} method, shown in Fig. 15, considering the V-V op-amp model from Fig. 2(a), yields different expressions for the return ratio if the loop is broken at the input or at the output of the op-amp—denoted here by $T_{AC\_IN}^{v-v}$ and $T_{AC\_OUT}^{v-v}$. One can easily demonstrate that $T_{AC\_IN}^{v-v}$ and T_{Bode}^{v-v} converge towards the same expression if the condition $Z_X \gg Z_Y$ is met:

$$\begin{aligned}T_{AC\_IN}^{vv}&=\frac{a_{VV}Z_LZ_G}{denom_{Z_Y}}+\frac{Z_Y}{Z_X}\xrightarrow{Z_X\gg Z_Y}\frac{a_{VV}Z_LZ_G}{denom_{Z_Y}};\\T_{Bode}^{vv}&=\frac{a_{VV}Z_LZ_G}{denom_{Z_Y}(1+Z_Y/Z_X)}\xrightarrow{Z_X\gg Z_Y}\frac{a_{VV}Z_LZ_G}{denom_{Z_Y}}.\end{aligned} \quad (25)$$

$T_{AC\_OUT}^{vv}$ converges to the same expression if $Z_X \gg Z_Y$. Note that the Z_X and Z_Y expressions are different for the two cases, therefore the condition $Z_X \gg Z_Y$ implies different constraints. In general this condition is met if the V-V op-amp input/output impedance has a very large/small value and the loop is broken at the input/output of the op-amp, respectively.

2) Simulation Results—Show-Case for Comparing the Methods: Let us analyze the circuit shown in Fig. 17, where the op-amp main open-loop parameters are: DC voltage gain 80 dB, main poles located at 550 Hz and 5 MHz, the output impedance $Z_{OUT}=100\ \Omega$ and the input impedance $Z_{IN}=1\ M\Omega$.

The frequency characteristics of the return ratios obtained by using the methods discussed here are shown in Fig. 18 along with the ratio of the impedances Z_X and Z_Y. The $L_{BIG}-C_{BIG}$ method provides the return ratio closest to the accurate one,

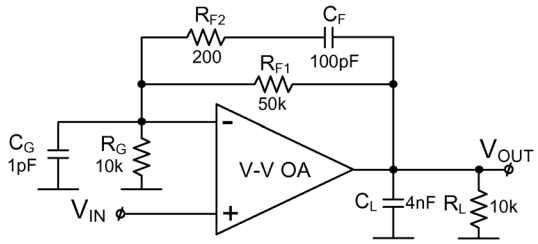

Fig. 17. Feedback circuit based on a standard V-V op-amp, used here to highlight the shortcomings of the approximate methods for finding T.

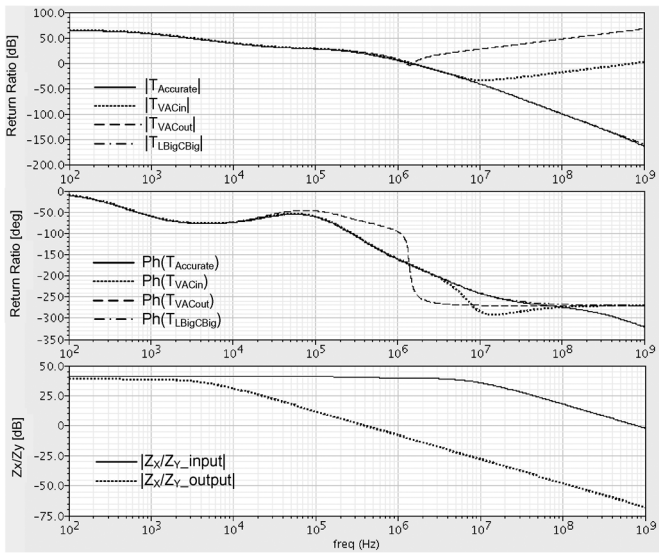

Fig. 18. Simulation results for the circuit shown in Fig. 17. Top and middle: module and phase characteristics of the return ratios yielded by the accurate methods (continuous line), the $\mathrm{V_{AC}}$ method applied at the OA input (dotted line) and output (dashed line) and the $\mathrm{L_{BIG}-C_{BIG}}$ method (dot-dashed line). Bottom: module of the $\mathrm{Z_X/Z_Y}$ ratio when the feedback loop is broken at the op-amp input (continuous line) and output (dotted line).

yielded by the STB analysis, followed by the $\mathrm{V_{AC}}$ method applied at the OA input. Both the module and phase characteristics provided by the later diverge from the accurate ones, but only at frequencies above $\mathrm{F_{0\ dB}}$ and $\mathrm{F_{-180^\circ}}$. Note that the ratio $\mathrm{Z_X/Z_Y}$ remains large up to these frequencies, too. When the feedback loop is broken at the OA output the ratio $\mathrm{Z_X/Z_Y}$ starts decreasing at a few kHz; the phase characteristic provided by $\mathrm{V_{AC}}$ method when applied at the OA output starts diverging significantly from the accurate one as soon as the ratio $\mathrm{Z_X/Z_Y}$ decreases below 20 dB. These results are in good agreement with the analytical analysis above.

Table I summarizes the phase- and gain- margin values yielded by the methods discussed here. Fig. 19 presents the step response of the same circuit, with slowly damped oscillations. This shape agrees with the phase margin yielded by the accurate methods (6.84°) and disagrees with the larger value given by the $\mathrm{V_{AC}}$ method applied at the op-amp output (60.24°). Note that the step response is determined solely by T, as the direct transmission—from the input to the output of the circuit, outside the feedback loop—is negligible in this case.

B. Feedback Circuits Based on CFB-OAs

The analytical analysis of the test circuits required by the $\mathrm{V_{AC}}$ and $\mathrm{L_{BIG}-C_{BIG}}$ methods, shown in Figs. 15 and 16, after

TABLE I
THE UNITY-RETURN RATIO FREQUENCY, THE PHASE AND GAIN MARGINS OBTAINED FOR THE CIRCUIT SHOWN IN FIG. 17 BY USING THE METHODS FOR FINDING THE RETURN RATIO THROUGH SIMULATIONS ANALYZED HERE

Method	$\mathrm{F_{0dB}}$ [MHz]	Phase Margin [degrees]	Gain Margin [dB]
Accurate	1.39	6.84	3.3
$\mathrm{V_{AC}}$ input	1.39	7	3.3
$\mathrm{V_{AC}}$ output	1.25	60.24	4.31
$\mathrm{L_{BIG}}$-$\mathrm{C_{BIG}}$	1.39	6.78	3.3

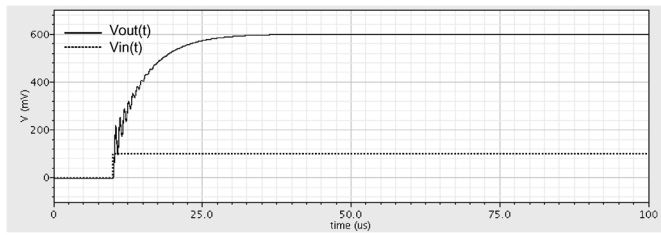

Fig. 19. Step response of the circuit shown in Fig. 17: the output voltage is drawn with continuous line, the input step voltage is drawn with dashed line.

replacing the generic op-amp there with the standard CFB-OA model shown in Fig. 2(b), yields three distinct return ratio expressions, $T^{i-v}_{AC\_IN}$, $T^{i-v}_{AC\_OUT}$ and $T_{L_{Big}} - C^{i-v}_{Big}$, all different from the accurate one given by (20). As discussed above, they converge mathematically towards the same expression as T^{i-v}_{Bode} if $\mathrm{Z_X} \gg \mathrm{Z_Y}$. However, considering the $\mathrm{Z_X}$ and $\mathrm{Z_Y}$ expressions corresponding to the $\mathrm{L_{BIG}-C_{BIG}}$ and the $\mathrm{V_{AC}}$ method applied at the op-amp input as given by (21), and the low input impedance of the CFB-OA, it results that the condition $\mathrm{Z_X} \gg \mathrm{Z_Y}$ is practically impossible to meet for real-life cases. Thus, large errors are to be expected when using these methods for feedback circuits based on CFB-OA. By analyzing the $\mathrm{Z_X}$ and $\mathrm{Z_Y}$ expressions corresponding to the $\mathrm{V_{AC}}$ method applied at the op-amp output given by (22) one can see that meeting the condition $\mathrm{Z_X} \gg \mathrm{Z_Y}$ is possible if the output impedance of the CFB-OA remains low enough over the required frequency range (up to and above the largest of the $\mathrm{F_{0\ dB}}$ and $\mathrm{F_{-180^\circ}}$). Only in these situations the $\mathrm{V_{AC}}$ method can be expected to be reasonably accurate.

C. Feedback Circuits Based on OTAs

For real-life circuits, with OTAs having large input and output impedances, the condition $\mathrm{Z_X} \gg \mathrm{Z_Y}$ can be met only for the $\mathrm{Z_X}$ and $\mathrm{Z_Y}$ expressions given by (21) and not by (22). Therefore, only the $\mathrm{L_{BIG}-C_{BIG}}$ and the $\mathrm{V_{AC}}$ method applied at the OTA input can possibly yield valid results.

D. Feedback Circuits Based on Current-Current Op-Amps

In this case, the condition $\mathrm{Z_X} \gg \mathrm{Z_Y}$ is practically impossible to meet for real-life op-amps, which have low input impedances and high output impedances:

$$\lim_{Z_{IN}\to 0} T^{i-i}_{AC\_IN} = \infty;\ \lim_{Z_{OUT}\to \infty} T^{i-i}_{AC\_OUT} = \infty;$$
$$\lim_{Z_{IN}\to 0} T^{i-i}_{L_{BIG}-C_{BIG}} = \infty \tag{26}$$

E. Summary of Main Comparison Points

Table II summarizes the conditions for which the $\mathrm{V_{AC}}$ and $\mathrm{L_{BIG}-C_{BIG}}$ methods can yield reasonable approximations,

TABLE II
CONDITIONS FOR WHICH V_{AC} AND $L_{Big} - C_{Big}$ METHODS MAY YIELD PRECISE

Method / OA type	V_{AC} applied at the OA input & L_{Big}-C_{Big}	V_{AC} applied at the OA output
V-V	$Z_{IN} \gg Z_G \| (Z_F+Z_L \| Z_{OUT})$	$Z_{OUT} \ll Z_L \| (Z_F+Z_G \| Z_{IN})$
I-V	Not suitable	$Z_{OUT} \ll Z_L \| (Z_F+Z_G \| Z_{IN})$
V-I	$Z_{IN} \gg Z_G \| (Z_F+Z_L \| Z_{OUT})$	Not suitable
I-I	Not suitable	Not suitable

TABLE III
COMPARISON BETWEEN THE ANALYZED METHODS

Method & Section in this paper	Validity or accuracy	No. of sim runs/circuit instantiations	Post-sim processing	Loading of the test points
Middlebrook (III.A)	Unilateral	2	Medium	N/A
Rosenstark (III.B)	Unilateral	2	Medium	Open-circuit or grounded
S-params (III.C)	Unilateral	1	Large	Set by user
Tian (IV.A)	Bilateral	2	Large	N/A
GFT (IV.B)	Bilateral	2	Large	N/A
Ochoa (IV.C)	Bilateral	2	Medium	Open-circuit or grounded
Current stimuli (IV.D)	Bilateral	2	Medium	Open-circuit
Wangenheim with extension (IV.E)	Bilateral	Set of sim runs	Small	N/A
V_{AC} (V.A)	Zx>>Zy	1	Small	N/A
L_{Big}-C_{Big} (V.B)	Zx>>Zy	1	Small	Open-circuit & grounded

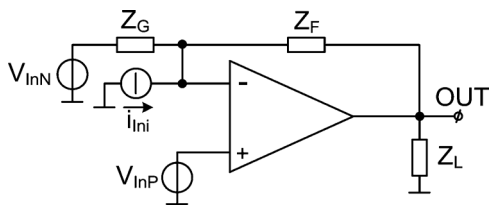

Fig. 20. An extension of the circuit shown in Fig. 1(b), that has two voltage inputs (V_{InP} and V_{InM}) and a current input (i_{Ini}). Its small-signal equivalent with the signal sources turned passive is the same as for the Fig. 1(b) circuit.

while Table III presents the main comparison points for all methods.

VII. EXTENSION TO OTHER CLASSES OF FEEDBACK CIRCUITS

A. Circuits With Multiple Inputs, Both Voltage and Current

The circuit presented in Fig. 20 was derived from the circuit analyzed so far, shown in Fig. 1(b), by adding to it a current input, i_{InI}, and a second voltage input, v_{InN}. This way, both the noninverting and inverting configurations of the op-amp are represented, as well as the simple current-to-voltage converter.

Obviously, the small-signal equivalent of this circuit when all signal sources are turned passive is exactly the same as the one obtained for the circuit shown in Fig. 1(b), for the same conditions. Thus, these circuits will have the same return ratio.

It follows that the results obtained and the conclusions drawn so far by analyzing circuits based on the one shown in Fig. 1(b), can be extended to the circuit presented in Fig. 20.

B. Differential Return Ratio of Fully Differential Circuits

The analysis can be further extended to fully differential (differential-input, differential output) op-amp-based circuits with reciprocal feedback networks, as their small-signal equivalent half-circuits for differential- and common-mode operation [3], [4], [9], with passivated signal sources, can be reduced to the topology shown in Fig. 1(b). All the methods described in Sections III and IV, except the $L_{BIG} - C_{BIG}$ method, can be applied directly to such fully differential circuits by following the procedure introduced in [9]: choose two symmetrical points at which both the differential- and common-mode feedback loops can be broken, then apply purely differential/common-mode test signals and derive the differential/common-mode return ratios by using the expressions corresponding to the method employed.

Examples and testbenches for deriving T through AC simulations by using Middlebrook's and V_{AC} methods for can be found in [9].

VIII. SUMMARY AND CONCLUSIONS

Ten methods for deriving through simulations the phase and module margins of feedback circuits have been compared: the classical ones introduced by Middlebrook, Rosenstark, Tian; more recent proposals from von Wangenheim and Ochoa; three methods popular within the industry: S-parameters, the V_{AC}, and $L_{BIG} - C_{BIG}$ methods; and a novel method that employs only current stimuli. They were split into three categories, considering the type of circuits their validity was proven for: accurate for bilateral or unilateral circuits and approximate.

The discussion was focused on, but not limited to, op-amp-based circuits with reciprocal feedback networks. All four op-amp types currently available commercially have been considered. The test setups and the related equations employed by each method were presented. The compliance with the requirement that the return ratio of a circuit should not depend on the point it was measured (the point the feedback loop was broken at and/or test stimuli were applied to) was assessed.

For the approximate methods, V_{AC} and $L_{BIG} - C_{BIG}$, the analysis included the conditions for which they could be expected to provide reasonably accurate results. It was proven analytically that the return ratios yielded by them and their "ideal" counterpart converge mathematically towards the same expression, if an inequality between the impedances seen from the test points along the loop is maintained up to a frequency higher than the largest of $F_{0\ dB}$ and $F_{-180°}$. The situations this condition can be met by real-life circuits were discussed. The limitations indicated by the analytical analysis were highlighted by simulations run on a show-case circuit.

The main points for comparing the accurate methods were:

- The number of simulation runs or circuit instantiations and the subsequent data processing they require: the S-parameter method requires only one run, while most of the other methods require two; however, post-sim processing is quite substantial. Von Wangenheim's method requires sets of simulations in order to reduce the interpolation error.
- Loading of the test points: Rosenstark's and Ochoa's methods require the test points to be left open-circuit and/or shorted to ground; the S-parameter method allows the user to set the impedances seen at the test point,

after breaking the feedback loop; the other methods minimize the impact their test stimuli have on the circuit impedances. The later can be extended to large-signal analysis—for example, Tian's method was used by Cadence to develop the STB (small-signal) and the P-STB (periodic-steady state) analyses.

The novel method presented in Section IV-D was devised following Ochoa's approach but requires simpler test setups that Ochoa and reduces the loading of the test points. It was demonstrated that this method is valid for bilateral circuits.

As von Wangenheim's method deals only with the phase-margin an extension was proposed for finding the gain-margin.

Finally, the analysis was extended to circuits with multiple voltage and current inputs and fully-differential circuits.

REFERENCES

[1] H. W. Bode, "Network Analysis and Feedback Amplifier Design," *Bell Teleph. Lab. Ser.*, Jul. 1945.

[2] S. Rosenstark, "A simplified method of feedback amplifier analysis," *IEEE Trans. Educ.*, vol. E-17, no. 4, pp. 192–198, 1974.

[3] P. R. Gray, P. J. Hurst, S. H. Lewis, and R. G. Meyer, *Analysis and Design of Analog Integrated Circuits*. Hoboken, NJ, USA: Wiley, 2001, ch. 8, 9.

[4] A. Sedra and K. Smith, *Microelectronic Circuits*. New York: Holt, Rinehart and Winston, 1987.

[5] P. J. Hurst, "A comparison of two approaches to feedback circuit analysis," *IEEE Trans. Educ.*, vol. 35, no. 3, pp. 253–261, 1992.

[6] H. T. Russell, "A loop-breaking method for the analysis and simulation of feedback amplifiers," *IEEE Trans. Circuits Syst. I, Fundam. Theory Appl.*, vol. 49, no. 8, pp. 1045–1061, Aug. 2002.

[7] R. Middlebrook, "Measurement of loop gain in feedback systems," *Int. J. Electron. Theory*, vol. 38, no. 4, pp. 485–512, 1975.

[8] S. Rosenstark, "Loop gain measurement in feedback amplifiers," *Int. J. Electron.*, vol. 57, no. 3, pp. 415–421, 1984.

[9] P. Hurst and S. Lewis, "Determination of stability using return ratios in balanced fully differential feedback circuits," *IEEE Trans. Circuits Syst. II, Analog Digit. Signal Process.*, vol. 42, no. 12, pp. 805–817, 1995.

[10] Y. Chiu, "Demystifying bilateral feedback analysis," in *Proc. IEEE 11th Int. Conf. Solid-State Integr. Circuit Technol.*, Oct. 2012, pp. 1–4.

[11] R. Middlebrook, "The general feedback theorem: A final solution for feedback systems," *IEEE Microw. Mag*, vol. 7, no. 2, pp. 50–63, 2006.

[12] M. Tian, V. Visvanathan, J. Hantgan, and K. Kundert, "Striving for small-signal stability," *IEEE Circuits Devices Mag.*, vol. 17, no. 1, pp. 31–41, 2001.

[13] A. Ochoa, "Loop gain in analog design—A new and complete approach," in *Proc. IEEE 55th Int. Midwest Symp. Circuits Syst. (MWSCAS)*, 2012, pp. 742–745.

[14] L. von Wangenheim, "Phase margin determination in a closed-loop configuration," *Circuits Syst. Signal Process.*, vol. 31, no. 6, pp. 1917–1926, Jun. 2012.

[15] S. Franco, *Design With Operational Amplifiers and Analog Integrated Circuits*. Boston, MA, USA: McGraw-Hill, 2002.

[16] G. Roberts and A. Sedra, *SPICE*. Oxford, U.K.: Oxford Univ. Press, 1996.

[17] Cadence Designs Systems Inc., Virtuoso Analog Design Environment L IC 6.1.4—User Guide 2009.

[18] F. Wiedmann, Loop Gain Simulation [Online]. Available: https://sites.google.com/site/frankwiedmann/loopgain

[19] M. Neag, R. Onet, and M. D. Topa, "Analysing the stability of circuits based on operational amplifiers by using frequency-domain simulations," *Acta Tech. Napocensis, Electron. Telecommun.*, vol. 51, no. 2, pp. 46–54, 2010.

Marius Neag received the Electronic Engineer Diploma from the Technical University of Cluj-Napoca, Romania, in 1991 and was awarded the Ph.D. degree by the University of Limerick, Ireland, in 1999. After working several years in Ireland and the U.S. as a Senior Designer of RF, analog and mixed-signal ICs he returned to the Technical University of Cluj-Napoca, where he lectures on the design of RF, analog, and mixed-signal ICs.

Raul Oneț received the Electronic Engineer Diploma and the Ph.D. degree from the Technical University of Cluj-Napoca, Romania, in 2008 and 2011, respectively. Since 2011 he has been an Associate Lecturer at the Technical University of Cluj-Napoca. His research areas include circuit theory and the design of integrated transceivers.

István Kovács received the M.Sc. degree in electrical engineering from the Technical University of Cluj-Napoca, Romania, in 2011. Since then he has been a Ph.D. student with the Digitally Enhanced RF and Analog IC Design Research Group at the same university. His research focuses on RF circuits for integrated transceivers.

Paul Mărtari received the M.Sc. degree in electrical engineering from the Technical University of Cluj-Napoca, Romania, in 2013, then started a Ph.D. program with the Digitally Enhanced RF and Analog IC Design Research Group at the same university. His research areas include the analysis and design of integrated circuits for power management and systems for energy conversion.